PCCP

ROYAL SOCIETY OF CHEMISTRY

CORRECTION

View Article Online
View Journal | View Issue

Cite this: *Phys. Chem. Chem. Phys.*, 2023, **25**, 24163

Correction: Increasing ion yield circular dichroism in femtosecond photoionisation using optimal control theory

Manel Mondelo-Martell,[a] Leon A. Kerber,[a] Daniel Basilewitsch,†[a] Hendrike Braun,[b] Christiane P. Koch[a] and Daniel M. Reich*[a]

DOI: 10.1039/d3cp90169f

rsc.li/pccp

Correction for 'Increasing ion yield circular dichroism in femtosecond photoionisation using optimal control theory' by Manel Mondelo-Martell *et al.*, *Phys. Chem. Chem. Phys.*, 2022, **24**, 9286–9297, https://doi.org/10.1039/D1CP05239J.

The authors have detected two issues in the numerical simulations reported in the originally published version of the article. First, the values of the electric and magnetic transition moments, obtained from quantum chemistry calculations were not sufficiently converged. Second, there was a mistake in the implementation of the rotational averaging in the model. After fixing these errors and choosing an improved optimisation functional, new simulations yield quantitatively different results. However, the physical mechanisms of the optimised pulses identified in the original paper remain valid. Here, the authors summarise the origin of the errors in the original publication and present newly converged energies, permanent and transition moments, as well as corrected figures and conclusions. Specifically, Tables 1 and 2 in the original article have been replaced with the corresponding tables in this correction, and Fig. 2–5 in the original article by Fig. 1–4 in this correction respectively. The authors also introduce and explain the new functional that has been used to optimise the pulse.

1 New *ab initio* data

Additional electronic structure calculations on fenchone have revealed that the basis set used in the original article (6-31G) was insufficient to correctly represent the system. The authors have therefore performed additional calculations with correlation consistent basis sets, following previous work.[1] The results that have been obtained using a cc-pVTZ basis set are summarised in Table 1. Compared to the parameterisation in the original article, the two main differences are the overall excitation energy (from 4.04 eV to 4.44 eV) and the qualitative changes in the y and z components of the electric dipole transition moment. Since the circular dichroism is, to first order, given by the overlap between magnetic and electric dipole transition moments, these changes cause qualitative differences to the behaviour of the system upon irradiation.

2 Description of the coding mistake in the original article and the solution

The error in the numerical code originated in the implementation of the negative sign accompanying the x component of the magnetic transition moment in the Hamiltonian (eqn (7) in the original article). There, the sign was included as a part of the x component during the rotation operations that generate the ensemble for the rotational averaging, but it should have only been present in the final expression of the Hamiltonian. After fixing this, as seen in Fig. 1, the g factor in the simulations with a circularly polarised guess pulse is ≈ 0.7, significantly higher than the previous value of 0.06, which coincidentally was in close agreement with experimental data.[2]

[a] *Dahlem Center of Complex Quantum Systems & Department of Physics, Freie Universität Berlin, Berlin, Germany. E-mail: christiane.koch@fu-berlin.de, danreich@zedat.fu-berlin.de*

[b] *Institute of Physics, Universität Kassel, Kassel, Germany. E-mail: braun@physik.uni-kassel.de*

† Present address: Institut für Theoretische Physik, Universität Innsbruck, Germany. E-mail: daniel.basilewitsch@uibk.ac.at

Table 1 Energies, permanent electric dipole and transition multipole moments for the ground and first electronic excited state of fenchone obtained at CCSD/cc-pVTZ level with DALTON2020.0

	$\|0\rangle$				$\|1\rangle$			
	Energy (eV)	El. dip. (ea_0)	Mag. dip. (μ_B)	El quad. (ea_0^2)	Energy (eV)	El. dip. (ea_0)	Mag. dip. (μ_B)	El quad. (ea_0^2)
$\langle 0\|$	0	$\begin{pmatrix}-0.066\\-1.119\\-0.451\end{pmatrix}$		$\begin{pmatrix}4.351 & 0.046 & -0.202\\0.046 & -5.863 & -3.574\\-0.202 & -3.574 & 1.512\end{pmatrix}$		$\begin{pmatrix}-0.0036\\-0.0052\\-0.0121\end{pmatrix}$	$\begin{pmatrix}-0.094\\-0.965\\-0.451\end{pmatrix}$	$\begin{pmatrix}0.161 & 0.798 & -1.638\\0.798 & -0.073 & -0.383\\-1.638 & -0.383 & -0.088\end{pmatrix}$
$\langle 1\|$	4.44	$\begin{pmatrix}-0.0036\\-0.0052\\-0.0121\end{pmatrix}$	$\begin{pmatrix}0.094\\0.965\\0.451\end{pmatrix}$	$\begin{pmatrix}0.161 & 0.798 & -1.638\\0.798 & -0.073 & -0.383\\-1.638 & -0.383 & -0.088\end{pmatrix}$		$\begin{pmatrix}-0.097\\-0.936\\-0.387\end{pmatrix}$		$\begin{pmatrix}4.713 & -0.631 & 0.336\\-0.631 & -4.791 & -2.021\\0.336 & -2.021 & 0.078\end{pmatrix}$

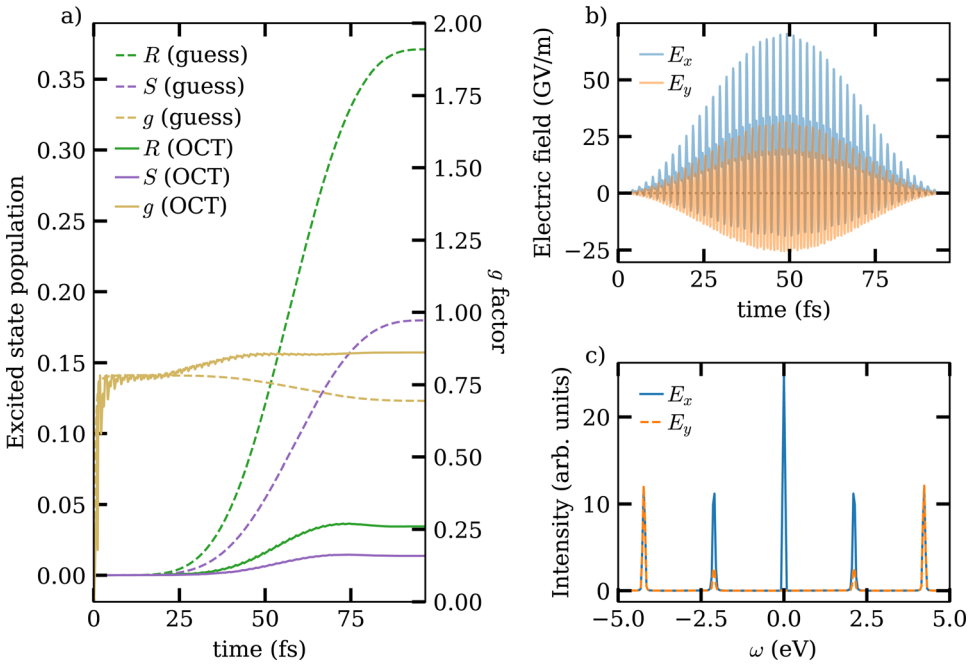

Fig. 1 Results for the optimisation of circular dichroism of a rotational ensemble for the A-band transition of fenchone. (a) Evolution of the excited-state population as a function of time for the *R* (green) and *S* (purple) enantiomer of fenchone, as well as the corresponding value of the anisotropy parameter *g* (yellow, in the right *y* axis). The dashed line corresponds to the circularly polarised guess pulse, while the solid line corresponds to the optimised control fields. The oscillations of *g* at short times are a numerical artifact due to the near 0 absorption of the excited states during the first femtoseconds. (b) Optimised pulses in time domain. (c) Optimised pulses in frequency domain.

The authors attribute the discrepancy between the currently calculated and experimental *g* value to neglecting the vibrational substructure of the electronic bands. In a real system, different geometries beyond the minimum of the electronic ground state potential energy surface contribute to the absorption even for the vibrational ground state. The corresponding nuclear displacements can be seen as perturbations to the equilibrium system, mixing its eigenstates, which leads to an intensity borrowing mechanism.[3,4] Particularly for the n → π* transition in carbonyl groups, these vibrational structure effects are known to be important.[4–6] This transition is very weak and thus the impact of mixing with electric dipole allowed transitions is comparatively large. As a result, the neglection of vibrational structure is a limitation of the model that the authors aim to address in a future study.

The functional used in the original manuscript, eqn (11), was designed to maximise the absolute difference in population,

$$J_T^{\text{old}} = 1 - \frac{1}{2}\left(\left|\langle \Psi^1 | \Psi_R(T)\rangle\right|^2 + \left|\langle \Psi^0 | \Psi_S(T)\rangle\right|^2\right) = \frac{1}{2}(1 - \Delta n). \quad (1)$$

After amending these issues in the original manuscript, the authors have observed that the optimisation functional in the original article did not lead to an increase in the anisotropy factor anymore. After changing the optimisation target to the anisotropy itself, the optimisations were successful in increasing its value, but this came at the cost of a very small absolute population difference, which would lead to a vanishing signal in the experiment. Therefore, instead of directly optimising the anisotropy *g*, the weighting

Table 2 Parameters of the circularly polarised guess pulse (anisotropy g = 0.69 after orientational averaging) and the optimised pulse (anisotropy g = 0.86 after orientational averaging)

	Optimised pulse						Guess pulse					
	$E^{(0)}$ (GV m^{-1})	$E^{(1)}$ (GV m^{-1})	$E^{(2)}$ (GV m^{-1})	$\omega^{(1)}$ (eV)	$\omega^{(2)}$ (eV)	φ	$E^{(0)}$ (GV m^{-1})	$E^{(1)}$ (GV m^{-1})	$E^{(2)}$ (GV m^{-1})	$\omega^{(1)}$ (eV)	$\omega^{(2)}$ (eV)	φ
E_x	25.71	24.91	25.71	4.22	2.11	1.53	0.0	25.71	0.0	4.44	—	1.57
E_y	0.0	25.39	5.92	4.22	2.11		0.0	25.71	0.0	4.44	—	

factor $|\Delta n|^a$ with $a = \frac{\log_{10} 2}{4} \sim 0.075$ has been included, which allows movement of the optimisation towards very low overall absorptions to be avoided. These ideas lead to defining the following new optimisation functional,

$$J_T^{\text{new}} = 2 - |\Delta n|^a g. \tag{2}$$

The authors have chosen the particular form of eqn (2) such that the new functional strikes a balance between the optimisation of the relative population difference encoded by g and the absolute population difference encoded by $|\Delta n|$. Larger values of a favour the absolute signal strength $|\Delta n|$, smaller values of a favour the anisotropy g. The authors have repeated the optimisations with different values of a and found the above value $a \simeq 0.075$ to provide a good compromise. It is large enough to obtain solutions that provide appreciable signal strength, but small enough that the anisotropy still represents the primary optimisation goal. The authors have also confirmed that the qualitative nature of the results does not sensitively depend on the precise value of a chosen for the optimisation – for example, in the additional calculations, very similar optimisation results for values $a \in [0.06, 0.09]$ have been obtained.

With this new functional, the relation between the fidelity and the difference in excited-state population between R and S enantiomers (eqn (17) in the original article) is less direct. Therefore, for the purpose of Fig. 3 and 4, the population difference, Δn, has been directly plotted. This facilitates distinguishing whether a given pulse favours absorption in the R enantiomer (to which positive values of Δn are assigned) or the S enantiomer (negative values of Δn).

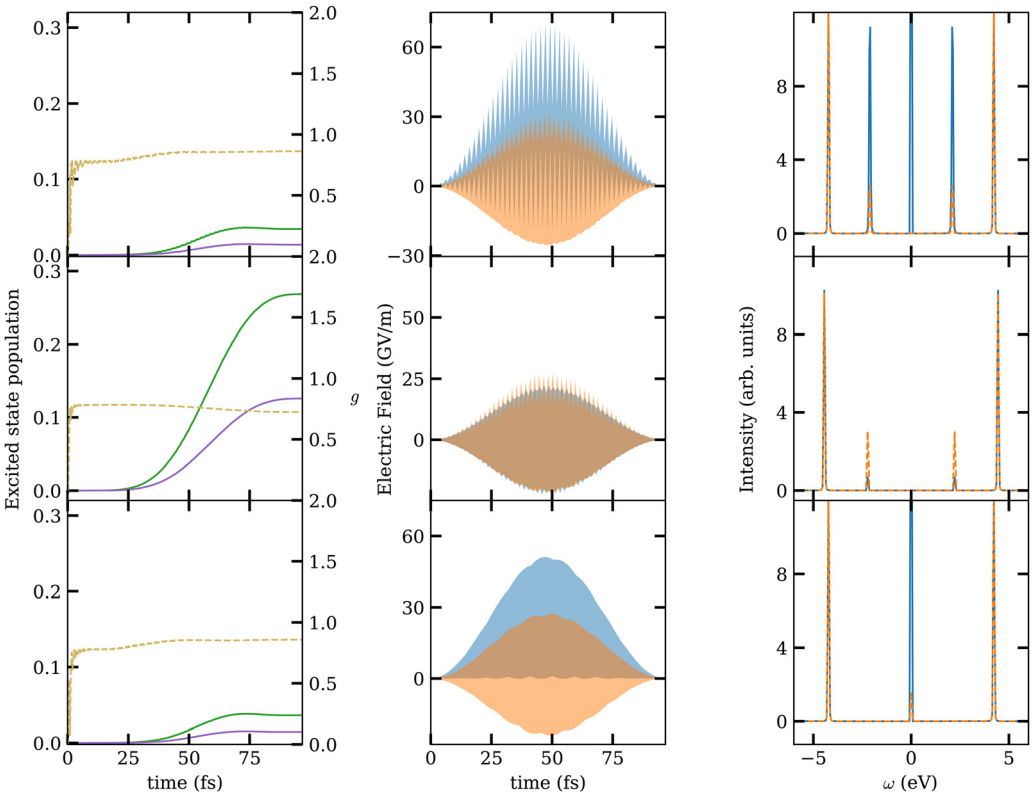

Fig. 2 Comparison of optimisations with a fully parametrised pulse (top), a restricted pulse without DC contribution (middle) and a restricted pulse without $\omega^{(2)}$ contribution (bottom). Left to right: excited-state population for the R (solid green) and S (solid purple) enantiomer and anisotropy factor g (dashed yellow, in right y axis); envelope of the optimised pulses in time domain; optimised pulses in frequency domain (E_x blue, E_y orange).

3 New optimisation results

Fig. 1 (taking the role of Fig. 2 from the original article) shows the excited-state population as a function of time for the *R* and *S* enantiomers, as well as the *g* factor, under irradiation with a circularly polarised pulse (dashed lines), respectively the optimised pulse (solid lines). With the new *ab initio* data and corrected code, an improvement of about 20% in the *g* factor (from $g = 0.69$ to $g = 0.86$) has been obtained using the new functional in eqn (2), although this comes at the cost of a reduced absolute absorption. The parameters of the optimised pulse are given in Table 2. The increase obtained is appreciably lower compared to the results from the original publication (from $g = 0.06$ to $g \approx 1$). Nonetheless, the model still predicts that it is possible to increase the anisotropy factor of fenchone using optimal control.

The population difference between the excited states of the *R* and *S* enantiomers irradiated with pulses optimised for each particular orientation is shown in Fig. 3. The predominance of light-coloured areas in this figure shows that for most orientations

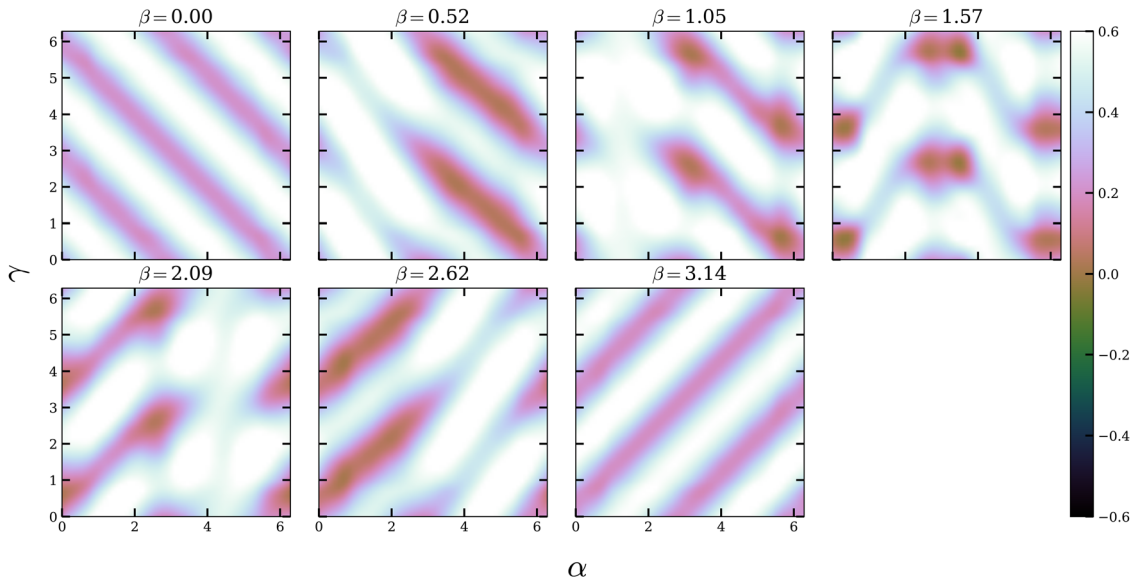

Fig. 3 Value of the difference in excited-state population between *R* and *S* enantiomers, Δn, optimised for individual orientations of fenchone as a function of the Euler angles α, β and γ.

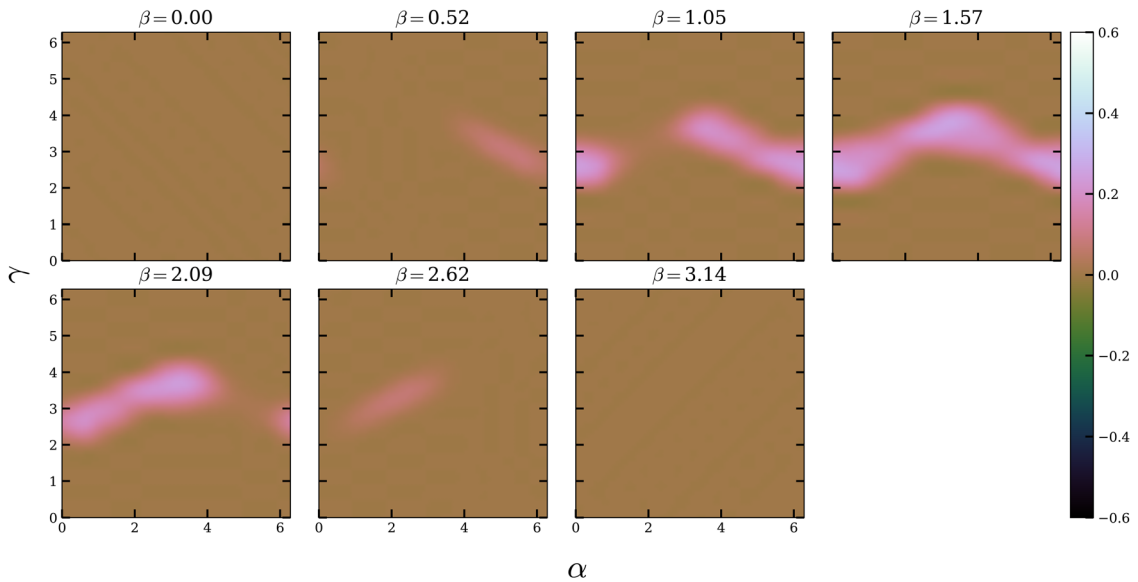

Fig. 4 Value of the difference in excited-state population between *R* and *S* enantiomers, Δn, after irradiation with the ensemble optimised pulse (Table 2 and Fig. 1) as a function of the Euler angles α, β and γ.

it is possible to find an optimal pulse that significantly increases the difference in excited-state population. This behaviour was similarly seen in Fig. 4 of the original article.

Fig. 4 shows the excited-state population difference between enantiomers when all orientations are irradiated with the optimised pulse shown in Fig. 1. Although the shape of the light-coloured areas indicating high chiral distinguishability is different from the previous results, *cf.* Fig. 5 of the original article, the crucial feature is preserved – the light-coloured areas are found predominantly in the panels close to $\beta = \pi/2$. This shows that the optimisation algorithm still focuses on increasing the population difference for those orientations that have a greater weight in the ensemble, as discussed in the original article.

The new simulations also confirm the importance of the DC contribution for the optimisation pulse. Analogously to the original article, this has been conformed by performing different pulse optimisations on the orientationally averaged system when considering different constraints to the pulse during the optimisation, namely: (i) forcing a null DC contribution to the field and (ii) forcing a null $\omega^{(2)}$ contribution to the field. The resulting excited-state population dynamics are shown in the middle (case (i)) and bottom panels (case (ii)) of Fig. 2, which corresponds to Fig. 3 in the original manuscript. In both old and new simulations, it is clear that the algorithm is not able to find a suitable pulse without a DC contribution, and that the electric quadrupole (coupling to the field predominantly with frequency $\omega^{(2)}$) only has a minor effect on the overall optimisation.

The Royal Society of Chemistry apologises for these errors and any consequent inconvenience to authors and readers.

References

1 R. E. Goetz, T. A. Isaev, B. Nikoobakht, R. Berger and C. P. Koch, *J. Chem. Phys.*, 2017, **146**, 024306.
2 F. Pulm, J. Schramm, J. Hormes, S. Grimme and S. D. Peyerimhoff, *Chem. Phys.*, 1997, **224**, 143–155.
3 G. Herzberg and E. Teller, *Z. Phys. Chem.*, 1933, **21B**, 410–446.
4 P. W. Atkins and R. S. Friedman, *Molecular Quantum Mechanics*, Oxford University Press, Oxford, 3rd edn, 1997.
5 W. Moffitt and A. Moscowitz, *J. Chem. Phys.*, 1959, **30**, 648–660.
6 *Circular Dichroism: principles and applications*, ed. K. Nakanishi, N. Berova and R. W. Woody, VCH, New York, 1994.